

Figure 1. Molecular structure of $[\text{Li}(\text{dme})_2][1,2,4,5-(\text{Me}_3\text{Si})_4\text{C}_6\text{H}_2]$ **2**: left, side view; right, top view (DME is omitted for the clarity). Selected bond lengths (Å) are as follows: C(1)–C(2) 1.558 (10), C(2)–C(3) 1.415 (11), C(3)–C(4) 1.392 (11), C(4)–C(5) 1.549 (11), C(5)–C(6) 1.411 (11), C(6)–C(1) 1.416 (11), C(1)–Si(1) 1.828 (8), C(2)–Si(2) 1.807 (8), C(4)–Si(3) 1.839 (8), C(5)–Si(4) 1.821 (8). Selected bond angles (deg) are as follows: C(6)–C(1)–C(2) 115.3 (6), C(1)–C(2)–C(3) 113.5 (6), C(2)–C(3)–C(4) 130.2 (6), C(3)–C(4)–C(5) 115.2 (6), C(4)–C(5)–C(6) 114.4 (6), C(5)–C(6)–C(1) 128.9 (7). Dihedral angle (deg) is as follows: C(1)–C(6)–C(5)/C(2)–C(3)–C(4) 8.0.

The ORTEP drawing of the molecular geometry of **2** is shown in Figure 1. The two lithium atoms are perfectly located above and below the center of the benzene ring, and each lithium atom is coordinated by one DME as a bidentate ligand. The distances between lithium atoms and the mean plane of the benzene ring are 1.870 (Li1) and 1.868 Å (Li2), and the distances between benzene carbons and lithium atoms are approximately equal (av 2.366 Å). The benzene ring is nearly planar as determined by the dihedral angle of 8° between C(1)–C(6)–C(5)/C(2)–C(3)–C(4) planes. The bond lengths of $\text{C}_{\text{ar}}\text{--Si}$ (av 1.824 Å) are shortened due to the increased bond order (cf. $\text{C}_{\text{ar}}\text{--Si}$ in Ph_4Si , 1.872 Å). The bond lengths of C(2)–C(3) (1.415 Å), C(3)–C(4) (1.392 Å), C(5)–C(6) (1.411 Å), and C(6)–C(1) (1.416 Å) are almost the same to average aromatic C–C bond distances (1.40 Å), whereas the bond lengths of C(1)–C(2) (1.558 Å) and C(4)–C(5) (1.549 Å) are appreciably elongated. The internal bond angles at C(1), C(2), C(4), and C(5) carbons range from 113.5 to 115.3°. However, the bond angles of both C(2)–C(3)–C(4) (130.2°) and C(5)–C(6)–C(1) (128.9°) are widened considerably. The molecular structure is in good accordance with that of the calculated (D_{2h}) form of $\text{C}_6\text{H}_6^{2-}$.^{5a} Thus the geometry of **2** reflects the nature of the ψ_{8s} LUMO of **1**.¹¹

In ^1H NMR spectrum of **2** in toluene- d_8 at 233 K, the signals due to the trimethylsilyl groups and aryl protons appear at 0.21 (36 H) and 5.11 ppm (2 H) together with the signals due to DME. In ^{13}C NMR, the aromatic carbons attached to the trimethylsilyl group can be observed at 80.8 ppm (1, 144.8 ppm), and the aromatic CH carbons can be seen at 161.8 ppm (1, 141.9 ppm). The former carbons exhibit a remarkable high field shift due to the location of the negative charge. ^{29}Si NMR resonances of the trimethylsilyl groups also shift to higher field (–19.2 ppm) compared to **1** (–3.3 ppm).

Of particular interest is ^7Li resonance at 10.7 ppm, being observed at the lowest magnetic field among the organolithium compounds reported so far.¹² The appreciable downfield shift is caused by the strong deshielding effect on the lithium atoms by the paratropic ring current resulting from 8π antiaromatic

system. On the basis of these spectroscopic properties, the molecular structure of **2** found in the crystals is retained in solution. Thus, the benzene dianion **2** has nearly the planar antiaromatic character with the anionic charge stabilized by the four silyl groups.

Acknowledgment. We are grateful for the financial support of the Ministry of Education, Science, and Culture of Japan (Specially Promoted Research No. 02102004).

Supplementary Material Available: X-ray experimental details and tables of positional parameters, thermal parameters, bond lengths, and angles (7 pages); table of observed and calculated structure factors (12 pages). Ordering information is given on any current masthead page.

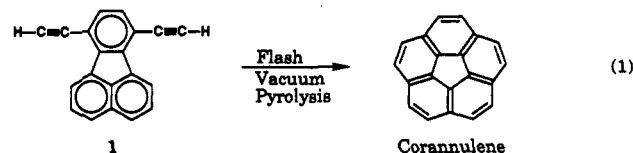
Corannulene. A Convenient New Synthesis¹

Lawrence T. Scott,*† Mohammed M. Hashemi,‡
Dayton T. Meyer,† and Hope B. Warren§

Department of Chemistry and Center for Advanced Study
University of Nevada, Reno, Nevada 89557-0020

Received June 24, 1991

We are pleased to report that corannulene, the marvelous bowl-shaped polycyclic aromatic hydrocarbon first prepared a quarter century ago by Barth and Lawton in a stunning tour de force,² is now readily accessible by a remarkably simple procedure (eq 1).



Our investigation of this high-temperature cyclization reaction was inspired by the pioneering work of R. F. C. Brown, who first

(11) It is known that the LUMO of **1** is ψ_{8s} by ESR study of the radical anion. Bock, H.; Kaim, W. *Z. Anorg. Allg. Chem.* **1979**, *459*, 103.

(12) For comparison, ^7Li signal of $[\text{Li}(\text{thf})_2](\text{Me}_3\text{Si})_4\text{C}_6$ was observed at –1.48 ppm owing to the nonaromaticity. In contrast to **2**, ^7Li of lithium cyclopentadienide (LiCp) was reported to be –8.60 ppm in Et_2O due to the strong shielding. See: (a) Elschenbroich, Ch.; Salzer, A. *Organometallics*; VCH Verlagsgesellschaft: Weinheim, 1989; pp 24–27. (b) Paquette, L. A.; Bauer, W.; Sivik, M. R.; Bühl, M.; Frigel, M.; Schleyer, P. v. R. *J. Am. Chem. Soc.* **1990**, *112*, 8776.

* University of Nevada, Reno, NV.

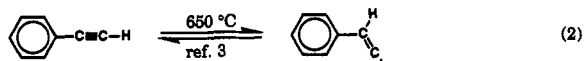
† Visiting scholar from Sharif University of Technology, Tehran, Iran.

‡ Undergraduate summer research student from California State University, Chico, CA.

(1) Thermal Rearrangements of Aromatic Compounds. 14. Part 13: Scott, L. T.; Roelofs, N. H. *Tetrahedron Lett.* **1988**, *29*, 6857–6860.

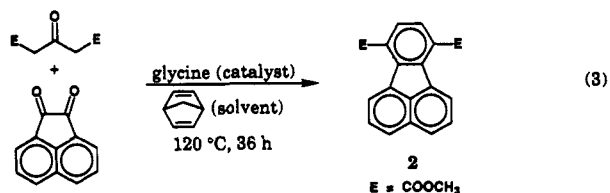
(2) Barth, W. E. Ph.D. Thesis, University of Michigan, 1966. Barth, W. E.; Lawton, R. G. *J. Am. Chem. Soc.* **1966**, *88*, 380–381. Barth, W. E.; Lawton, R. G. *J. Am. Chem. Soc.* **1971**, *93*, 1730–1745.

demonstrated the reversible rearrangement of terminal acetylenes to vinylidenes (e.g., eq 2) under conditions of flash vacuum pyrolysis (FVP).³ Of special significance was Brown's report that 2-ethynylbiphenyl, a subunit in 7,10-diethynylfluoranthene (**1**), cyclizes to phenanthrene under FVP conditions,⁴ apparently by trapping of the transient carbene via intramolecular C-H insertion. The concomitant formation of 1,2-benzazulene in that reaction provides compelling evidence for generation of a carbene intermediate, although the phenanthrene could conceivably arise by a competing electrocyclic pathway.⁵



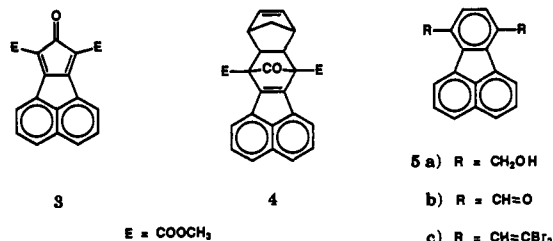
Numerous unsuccessful attempts to construct the corannulene ring system by conventional cyclizations of other 7,10-disubstituted fluoranthenes in solution have been recorded,^{6,7} and these failures have all been attributed to the inability of appendages on the upper ring to reach across the splayed-out bay region of the fluoranthene nucleus. The critical feature of our approach that obviates this problem is the high temperature employed. We reasoned that the ability of polycyclic aromatic hydrocarbons to fluctuate drastically away from their equilibrium geometries at high temperatures⁸ should allow the fluoranthene nucleus to fold like a hinge at the five-membered ring, thereby bringing the reactive centers from the otherwise remote upper and lower regions of the molecule into close proximity. To our knowledge, the isomerization in eq 1 is the first well-defined demonstration of a chemical reaction that captures a planar polycyclic aromatic hydrocarbon in a temporary nonplanar geometry to build a convex surface. It is not difficult to envisage applications of this principle to the elaboration of other curved molecular surfaces based on trigonal carbon lattices, e.g., spheroidal C₆₀.

Bis-acetylene **1** can be easily prepared in four steps from the known 7,10-fluoranthenedicarboxylic ester **2**,^{6,9} a key compound for which we have developed a new one-pot synthesis (eq 3).



The mechanism for this striking transformation presumably involves initial formation of cyclopentadienone **3** by a double Knoevenagel condensation, followed by an inverse electron demand Diels-Alder cycloaddition of norbornadiene, which serves both as the reaction solvent and as an acetylene equivalent in the cycloaddition. The unstable heptacyclic intermediate **4** then loses carbon monoxide and cyclopentadiene to unveil a fluoranthene ring system. The earlier synthesis of **2** entailed isolation of the reactive cyclopentadienone **3**, which was subsequently refluxed with norbornadiene in butanol.^{6,9} We have found that a change in the condensation catalyst allows these two steps to be neatly

telescoped into a single operation wherein cyclopentadienone **3** is trapped in situ to produce diester **2** more conveniently and in improved overall yield (49%) on a 20-g scale.



Reduction of diester **2** (lithium aluminum hydride, THF, 25 °C, 6 h) gave diol **5a** (95%),⁶ which was subsequently oxidized (pyridinium chlorochromate, THF, 25 °C, 5 h) to dialdehyde **5b** (70%).¹⁰ Conversion of the aldehyde groups in **5b** to 2,2-dibromovinyl groups according to the Corey-Fuchs recipe¹¹ (CBr₄, Ph₃P, Zn, CH₂Cl₂, 25 °C, 36 h; then **5b**, CH₂Cl₂, 25 °C, 5 h; then reflux 12 h) afforded **5c** in 50% yield.¹² Treatment of tetrabromide **5c** with lithium diisopropylamide (4.0 molar equiv, THF, -78 °C, 5 h) gave 7,10-diethynylfluoranthene (**1**)¹³ in 80% yield.

Flash vacuum pyrolysis of **1** was conducted in a commercially available Trahanovsky pyrolysis apparatus.¹⁴ At an oven temperature of 1000 °C, the material that passes through the pyrolysis tube cyclizes quantitatively to corannulene.¹⁵ Unfortunately, a substantial portion of the rather nonvolatile diacetylene suffers polymerization in the heated sample chamber before it can sublime, and we have so far been unable to improve the yield of corannulene from **1** to above ca. 10% on a 30–50-mg scale. In a typical run, 40 mg of **1** gave 4 mg of crystalline corannulene, which was already pure by GC (>99%) and ¹H NMR.

Luckily, the more robust tetrabromide **5c** also gives corannulene under FVP conditions (1000 °C, ca. 40% yield in preliminary experiments), conceivably via electrocyclic ring closure followed by aromatization and pyrolytic loss of bromine atoms. In one run, 30 mg of **5c** gave 5.1 mg of crystalline corannulene after chromatography. We are now turning our attention to optimization and scale-up of this even shorter route to corannulene.

The ¹³C NMR spectrum of corannulene has never been reported. We find, as expected, that it exhibits three signals (75 MHz, CDCl₃, δ 135.81, 130.84, and 127.18). The signal at δ 127.18 shows a strong one-bond C-H coupling (¹J_{CH} = 159.7 Hz), which confirms its origin as the 10 equivalent methine carbon atoms on the rim. Of the remaining two signals, only the one at 130.84 ppm shows a significant NOE, which allows us to assign it to the five quaternary carbon atoms on the rim, leaving the signal at 135.81 ppm assigned to the five quaternary carbon atoms of the hub.

We credit our success in this venture to Barth and Lawton,² Brown,^{3,4} Craig,⁶ Martin,⁸ and Trahanovsky,¹⁴ without whose shoulders to stand on we could never have seen this far. With corannulene now available, we have begun to explore its potentially fascinating chemistry, including its barrier to bowl inversion.

(3) Brown, R. F. C.; Harrington, K. J.; McMullen, G. L. *J. Chem. Soc., Chem. Commun.* **1974**, 123–124. Brown, R. F. C.; Eastwood, F. W.; Jackman, G. P. *Aust. J. Chem.* **1977**, *30*, 1757–1767. Brown R. F. C.; Eastwood, F. W.; Jackman, G. P. *Aust. J. Chem.* **1978**, *31*, 579–586. See also ref 4.

(4) Brown, R. F. C.; Eastwood, F. W.; Harrington, K. J.; McMullen, G. L. *Aust. J. Chem.* **1974**, *27*, 2393–2402.

(5) Phenanthrene, could also arise in this reaction via the known benzazulene-to-phenanthrene rearrangement: Alder, R.; Whitaker, G. *J. Chem. Soc., Perkin Trans. 2* **1975**, 714–723.

(6) Craig, J. T.; Robins, M. D. W. *Aust. J. Chem.* **1968**, *21*, 2237–2245.

(7) Jacobson, R. H. Ph.D. Dissertation, University of California, Los Angeles, 1986.

(8) See, for example, the classic helix racemization studies of Martin and Libert: Martin, R. H.; Libert, V. *J. Chem. Res., Miniprint* **1980**, 1940–1950 and references cited therein.

(9) The first synthesis of **2** was patterned after earlier work by Allen and Van Allen. Tucker, and Mackenzie: Allen, C. F. H.; Van Allen, J. A. *J. Org. Chem.* **1952**, *17*, 845–854. Tucker, S. H. *J. Chem. Soc.* **1958**, 1462–1465. Mackenzie, K. *J. Chem. Soc.* **1960**, 473–483.

(10) Dialdehyde **5b**: yellow crystals, mp 195–198 °C dec; ¹H NMR (300 MHz, CDCl₃) δ 7.71 (dd, 2 H, J = 7.2 and 8.1 Hz), 7.94 (s, 2 H), 8.00 (d, 2 H, J = 8.1 Hz), 8.71 (d, 2 H, J = 7.2 Hz), 10.71 (s, 2 H); high-resolution mass spectrum calcd for C₁₈H₁₀O₂, 258.0681, found 258.0688.

(11) Corey, E. J.; Fuchs, P. L. *Tetrahedron Lett.* **1972**, 3769–3772.

(12) Tetrabromide **5c**: colorless crystals from methanol, mp 188–190 °C; ¹H NMR (300 MHz, CDCl₃) δ 7.47 (s, 2 H), 7.69 (dd, 2 H, J = 6.9 and 8.1 Hz), 7.91 (d, 2 H, J = 8.1 Hz), 7.94 (d, 2 H, J = 6.9 Hz), 7.95 (s, 2 H); high-resolution mass spectrum calcd for C₂₀H₁₀Br₄, 565.7518, found 565.7517.

(13) 7,10-Diethynylfluoranthene (**1**): pale yellow crystals, mp 143–145 °C; ¹H NMR (300 MHz, CDCl₃) δ 3.63 (s, 2 H), 7.44 (s, 2 H), 7.67 (dd, 2 H, J = 6.9 and 9.0 Hz), 7.91 (d, 2 H, J = 9.0 Hz), 8.57 (d, 2 H, J = 6.9 Hz); high-resolution mass spectrum calcd for C₂₀H₁₀, 250.0782, found 250.0781.

(14) Our pyrolysis apparatus was purchased from Kontes, Inc., Vineland, NJ 08360; a good vacuum (ca. 10⁻⁴ Torr or better) is essential to facilitate sublimation of the corannulene precursor.

(15) At 750 °C, recovered diyne **1** constitutes 50% of the material in the trap, accompanied by 30% of the intermediate with just one new ring closed and 20% of corannulene. At 900 °C, starting material no longer survives, and the intermediate with only one new ring closed represents the major product, accompanied by lesser amounts of corannulene.

Acknowledgment. We thank the Department of Energy for financial support of this work. Special thanks are also extended

to Scott E. Carver for scaling up the one-step synthesis of fluoranthenedicarboxylic ester **2**.

Additions and Corrections

¹H NMR Spectroscopy and the Electronic Structure of the High Potential Iron-Sulfur Protein from *Chromatium vinosum* [*J. Am. Chem. Soc.* **1991**, *113*, 1237-1245]. IVANO BERTINI,* FABRIZIO BRIGANTI, CLAUDIO LUCHINAT, ANDREA SCOZZAFAVA, and MARCO SOLA

Pages 1243 and 1244: Figures 6A and 8A were printed incorrectly. The corrected figures and captions are given below.

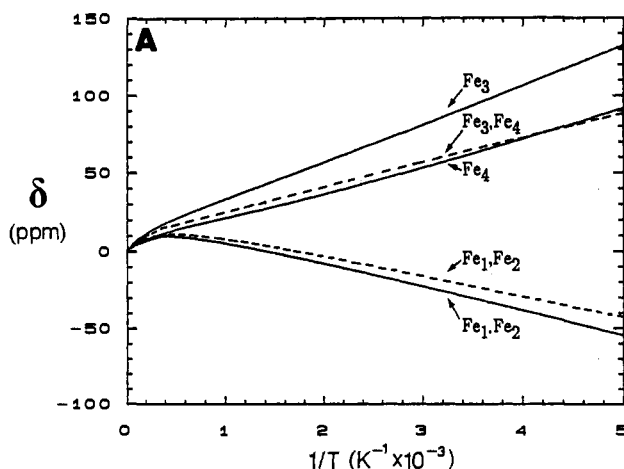


Figure 6. (A) Temperature dependence of the ¹H NMR isotropic shifts of oxidized HiPIP calculated by using eq 8 with $J = 300 \text{ cm}^{-1}$, $\Delta J_{12} = 100 \text{ cm}^{-1}$, $\Delta J_{34} = -100 \text{ cm}^{-1}$, and $B_{34} = 0 \text{ cm}^{-1}$ (—), or $J = 300 \text{ cm}^{-1}$, $\Delta J_{12} = 70 \text{ cm}^{-1}$, $\Delta J_{34} = 0 \text{ cm}^{-1}$, and $B_{34} = 300 \text{ cm}^{-1}$ (---) ($\text{Fe}_1 = \text{Fe}_2 = \text{Fe}_3 = \text{Fe(III)}$ and $\text{Fe}_4 = \text{Fe(II)}$, $S_{12} = 4$, $S_{34} = 9/2$ ground state).

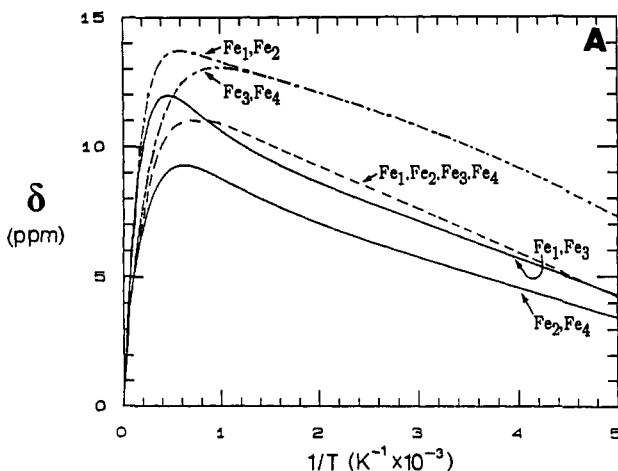


Figure 8. (A) Temperature dependence of the ¹H NMR isotropic shifts of reduced HiPIP calculated by using eq 8 with $J = 400 \text{ cm}^{-1}$, $\Delta J_{12} = \Delta J_{34} = -200 \text{ cm}^{-1}$, and $B_{12} = B_{34} = 0 \text{ cm}^{-1}$ (—), or $J = 400 \text{ cm}^{-1}$, $\Delta J_{12} = \Delta J_{34} = 0 \text{ cm}^{-1}$, and $B_{12} = B_{34} = 400 \text{ cm}^{-1}$ (---) ($\text{Fe}_1 = \text{Fe}_3 = \text{Fe(III)}$ and $\text{Fe}_2 = \text{Fe}_4 = \text{Fe(II)}$, $S_{12} = S_{34} = 9/2$ ground state), or $J = 200 \text{ cm}^{-1}$, $\Delta J_{12} = \Delta J_{34} = 200 \text{ cm}^{-1}$, and $B_{12} = B_{34} = 0 \text{ cm}^{-1}$ (—) ($\text{Fe}_1 = \text{Fe}_2 = \text{Fe(III)}$ and $\text{Fe}_3 = \text{Fe}_4 = \text{Fe(II)}$, $S_{12} = S_{34} = 0$ ground state). For each choice of parameters the upper curve corresponds to Fe(III) whereas the lower curve corresponds to Fe(II).